

DemMamba: Alignment-free Raw Video Demoiréing with Frequency-assisted Spatio-Temporal Mamba

Shuning Xu¹, Xina Liu, Binbin Song, Xiangyu Chen, Qiubo Chen, Jiantao Zhou

¹University of Macau

yc07425@um.edu.mo

Abstract

Moiré patterns, resulting from the interference of two similar repetitive patterns, are frequently observed during the capture of images or videos on screens. These patterns vary in color, shape, and location across video frames, posing challenges in extracting information from adjacent frames and preserving temporal consistency throughout the restoration process. Existing deep learning methods often depend on well-designed alignment modules, such as optical flow estimation, deformable convolution, and cross-frame self-attention layers, incurring high computational costs. Recent studies indicate that utilizing raw data as input can significantly improve the effectiveness of video demoiréing by providing the pristine degradation information and more detailed content. However, previous works fail to design both efficient and effective raw video demoiréing methods that can maintain temporal consistency and prevent degradation of color and spatial details. This paper introduces a novel alignment-free raw video demoiréing network with frequency-assisted spatio-temporal Mamba (DemMamba). It features sequentially arranged Spatial Mamba Blocks (SMB) and Temporal Mamba Blocks (TMB) to effectively model the inter- and intra-relationships in raw videos affected by moiré patterns. An Adaptive Frequency Block (AFB) within the SMB facilitates demoiréing in the frequency domain, while a Channel Attention Block (CAB) in the TMB enhances the temporal information interactions by leveraging inter-channel relationships among features. Extensive experiments demonstrate that our proposed DemMamba surpasses state-of-the-art methods by 1.3 dB in PSNR, and also provides a satisfactory visual experience.

1. Introduction

Moiré patterns appear as repetitive, wave-like, colorful distortions when capturing images or videos on screens. These patterns result from spatial frequency aliasing between the

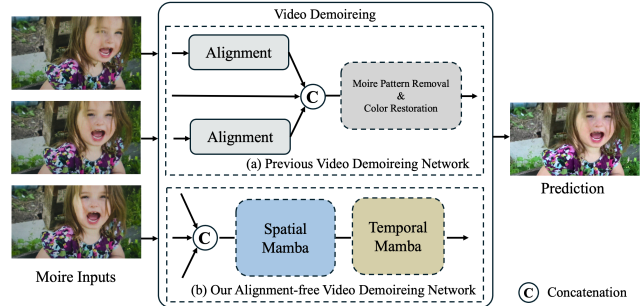


Figure 1. Motivation of our alignment-free raw video demoiréing network. (a) Most of the previous methods utilize a well-designed module for alignment. (b) We propose Spatial Mamba and Temporal Mamba for effective inter- and intra-relationship modeling.

color filter array of camera sensors and the LCD screen subpixels [39], leading to an unsatisfactory visual experience. Video demoiréing, compared to image demoiréing, poses greater challenges; it demands not only the restoration of high-quality, moiré-free frames with natural colors but also significant effort to maintain temporal consistency.

In recent years, many learning-based video demoiréing approaches [5, 6, 26, 32, 34, 47] have been proposed. Specifically, VDmoiré [6] establishes the first video demoiréing dataset captured with hand-held cameras and designs a baseline video demoiréing model that utilizes implicit feature space alignment and selective feature aggregation. DTNet [47] introduces a direction-aware, temporally guided network with bilateral learning for video demoiréing, employing both multi-scale architecture and deformable convolution for the alignment process. Many studies suggest that eliminating moiré patterns in the raw domain is more effective than in the sRGB domain [5, 48, 51], as moiré patterns in the raw domain are less pronounced due to the absence of nonlinear operations, such as gamma correction and demosaicing, typical in image signal processing (ISP), which often amplify these artifacts. Given the increasing availability of raw data in modern smartphones and DSLR cameras, demoiréing in the raw do-

main is both feasible and beneficial. RawVD [5] is a pioneering work that performs video demoiréing in the raw domain using a dual-branch convolution approach, which combines cross-channel and color-group convolutions to remove moiré patterns and enhance visual structures.

Most of the aforementioned video demoiréing methods rely heavily on well-designed modules, such as the pyramid cascading deformable (PCD) module proposed by EDVR [42], which uses deformable convolutions to align multiple frames, as depicted in Fig. 1(a). Although this approach appears to be straightforward, it incurs a high computational burden. This poses significant challenges to efficiency, particularly in processing high-resolution, long video sequences, hampering its application in modeling long-term inter- and intra-frame correlations. Recently, State Space Models (SSMs) [18], originating from control systems theory, have demonstrated advantages in natural language processing [9, 10] and computer vision [35, 58] due to their linear complexity in handling long sequences. In low-level vision, some works have extended the application of Mamba to image restoration [1, 7, 12, 21], effectively balancing the global receptive field and computational efficiency. This prompts us to further delve into the potential of Mamba in video restoration, particularly applying it to raw video demoiréing, aiming to efficiently remove moiré patterns while maintaining temporal consistency. To facilitate effective inter- and intra-relationship modeling in raw videos with moiré patterns, we propose the Spatial Mamba and Temporal Mamba modules, which are arranged sequentially, as demonstrated in Fig. 1(b).

In this paper, we propose an alignment-free raw video demoiréing network, termed DemMamba, featuring frequency-assisted spatio-temporal Mamba. Our principal design employs sequentially arranged Spatial Mamba Blocks (SMB) and Temporal Mamba Blocks (TMB) to effectively model inter- and intra-relationships, thereby efficiently removing moiré patterns while maintaining temporal consistency. For SMB and TMB, we adopt different scanning strategies and introduce additional modules to enhance correlations within the spatial and temporal domains, respectively. Considering the formation process of moiré patterns, we utilize a learnable compressor in the frequency domain to selectively attenuate frequencies associated with prominent moiré patterns in SMB. For TMB, channel attention is employed to further enhance temporal information interactions by exploiting inter-channel relationships among features.

In summary, our contributions are listed as follows:

- We adapt Mamba into a spatio-temporal framework for the video restoration task and design a frequency-assisted spatio-temporal Mamba network for raw video demoiréing. By alternately employing Spatial Mamba and Temporal Mamba blocks, DemMamba effectively al-

leviates moiré patterns and maintains temporal consistency in an alignment-free approach.

- SMB is utilized for the intra-frame demoiréing process. We introduce a learnable compressor to attenuate prominent moiré frequencies in the frequency domain.
- TMB is designed to capture inter-channel relationships, which facilitates better utilization of neighboring information and maintains temporal consistency. The temporal sequences are processed through simultaneous forward and backward SSMs, and channel attention is introduced to enhance the integration of temporal information.
- We conduct extensive experiments on both raw video and image demoiréing datasets. DemMamba surpasses state-of-the-art methods by 1.3 dB in PSNR, and also delivers a visually appealing result.

2. Related Works

2.1. Image and Video Demoiréing

Moiré patterns result from the interference between two similar frequency patterns, frequently appearing in screen captures and severely degrading the visual experience. Several learning-based solutions have been proposed to eliminate moiré patterns from images [4, 13, 14, 23–25, 28, 31, 37, 39, 40, 45, 48, 50, 55, 57]. Compared to image demoiréing, video demoiréing [6, 32, 34, 47] presents a greater challenge, as it requires generating temporally consistent moiré-free predictions. VDMoiré [6] introduces a straightforward video demoiréing model that leverages implicit feature space alignment and selective feature aggregation. Additionally, it incorporates a novel relation-based consistency loss to enhance temporal consistency across frames. DTNet [47] proposes a direction-aware, temporally guided bilateral learning network for video demoiréing, utilizing multi-scale alignment and deformable convolution during the alignment process. RawVD [5] employs a pyramid cascading deformable module for the alignment process and utilizes a dual-branch convolution approach that combines cross-channel and color-group convolutions to effectively remove moiré patterns and enhance visual structures. Notably, existing video demoiréing methods heavily rely on sophisticated alignment modules, which significantly increasing computational complexity. Therefore, we introduce DemMamba, an alignment-free method designed to effectively and efficiently eliminates moiré patterns from videos, maintaining temporal consistency while reducing computational demands.

2.2. Deep Raw Image and Video Restoration

Raw pixels provide richer information for visual tasks due to their broader bit depth, as they inherently contain a vast amount of data. Recently, several low-level vision tasks have adopted raw data, including low-light enhancement

ment [8, 15, 16], super-resolution [30, 46, 52], reflection removal [20, 36], and moiré pattern removal [5, 48, 51]. RRID [48] proposes an image demoiréing network that employs paired raw-sRGB data to facilitate the color recovery process. RawVD [5], the first work to explore raw video demoiréing, constructs the RawVDemoiré dataset. In this paper, considering that raw pixels offer more information and that moiré patterns are less apparent in the raw domain, we perform video demoiréing in the raw domain.

2.3. State Space Models

State Space Models (SSMs) [18] have garnered significant attention recently due to their notable efficiency in employing state space transformations to manage long-term dependencies in language sequences [11]. More recently, Mamba [9] is designed with a selective scan mechanism and an efficient hardware architecture, demonstrating substantial performance improvements. These advancements validate the effectiveness of Mamba in visual tasks, extending its applications to semantic segmentation [27, 38, 59], image classification [2, 29, 33, 49, 58], video understanding [3, 41], and image restoration [12, 19, 21, 22, 44, 56]. Building on Mamba’s success in these areas, this paper explores the potential of Mamba in raw video demoiréing. The frequency-assisted spatio-temporal design of our proposed DemMamba also presents an effective approach that could be adapted for other video restoration tasks.

3. Proposed Method

Moiré patterns, initially caused by frequency interference, are further exacerbated by the nonlinear processes in the ISP. Thus, introducing raw data for video demoiréing may provide greater effectiveness. The color, shape, and location of moiré patterns can vary across different frames due to changing camera viewpoints, automatic focal length adjustments, and other factors. Therefore, the demoiréing model must capture long-range dependencies in both spatial and temporal domains. This capability is essential for effectively leveraging global information from the current frame and relevant temporal information from adjacent frames to remove moiré patterns while ensuring temporal consistency across the video sequence.

In this work, we propose a frequency-assisted spatio-temporal Mamba for raw video demoiréing. The Spatial Mamba Block (SMB) and Temporal Mamba Block (TMB) are sequentially arranged to model intra- and inter-relationships in raw videos affected by moiré patterns.

3.1. Preliminaries

The recent advancements in structured state-space sequence models (S4) are largely inspired by the continuous linear time-invariant (LTI) systems, which map a 1-dimensional input function or sequence $x(t) \in \mathbb{R}$ to an output $y(t) \in$

\mathbb{R} through an implicit latent state $h(t) \in \mathbb{R}^N$. Formally, this system can be described by a linear ordinary differential equation (ODE):

$$\begin{aligned} h'(t) &= \mathbf{A}h(t) + \mathbf{B}x(t), \\ y(t) &= \mathbf{C}h(t) + \mathbf{D}x(t), \end{aligned} \quad (1)$$

where N denotes the state size, $\mathbf{A} \in \mathbb{R}^{N \times N}$, $\mathbf{B} \in \mathbb{R}^{N \times 1}$, $\mathbf{C} \in \mathbb{R}^{1 \times N}$, and $\mathbf{D} \in \mathbb{R}$.

Subsequently, the discretization process is typically employed to integrate Eq. 1 within practical deep learning algorithms. Specifically, let Δ denote the timescale parameter to transform the continuous parameters \mathbf{A}, \mathbf{B} to discrete parameters $\bar{\mathbf{A}}, \bar{\mathbf{B}}$. The most commonly used method for discretization is the zero-order hold (ZOH) rule, which is formulated as:

$$\begin{aligned} \bar{\mathbf{A}} &= \exp(\Delta \mathbf{A}), \\ \bar{\mathbf{B}} &= (\Delta \mathbf{A})^{-1}(\exp(\mathbf{A}) - \mathbf{I}) \cdot \Delta \mathbf{B}. \end{aligned} \quad (2)$$

After the discretization, the discrete version of Eq. 1 with step size Δ can be rewritten in the following RNN form:

$$\begin{aligned} h_k &= \bar{\mathbf{A}}h_{k-1} + \bar{\mathbf{B}}x_k, \\ y_k &= \mathbf{C}h_k + \mathbf{D}x_k. \end{aligned} \quad (3)$$

Furthermore, Eq. 3 can also be equivalently transformed into the following CNN form mathematically:

$$\begin{aligned} \bar{\mathbf{K}} &\triangleq (\mathbf{C}\bar{\mathbf{B}}, \mathbf{C}\bar{\mathbf{A}}\bar{\mathbf{B}}, \dots, \mathbf{C}\bar{\mathbf{A}}^{L-1}\bar{\mathbf{B}}), \\ \mathbf{y} &= \mathbf{x} \circledast \bar{\mathbf{K}}, \end{aligned} \quad (4)$$

where L denotes the length of the input sequence, \circledast is convolution operation, and $\bar{\mathbf{K}} \in \mathbb{R}^L$ represents a structured convolution kernel.

Building on S4’s framework, the recent advanced state-space model, Mamba [9], has further improved $\bar{\mathbf{B}}, \mathbf{C}$, and Δ to be input-dependent, thereby enabling dynamic feature representations. Mamba’s approach to image restoration leverages the same recursive form of Eq. 3, allowing the model to capture long sequences, thus aiding in pixel-wise restoration. Additionally, the parallel scan algorithm [9] allows Mamba to enjoy the same advantages of parallel processing as Eq. 4, thus facilitating efficient training.

3.2. Architecture

Fig. 2 demonstrates an overview of the proposed DemMamba for raw video demoiréing. Given three consecutive raw moiré frames $\{\mathbf{I}_{\text{raw}}^{t-1}, \mathbf{I}_{\text{raw}}^t, \mathbf{I}_{\text{raw}}^{t+1}\}$, the objective of raw video demoiréing is to restore the reference frame $\mathbf{I}_{\text{raw}}^t$ to a clean output in the sRGB domain, denoted as $\hat{\mathbf{I}}_c^t$. The complete pipeline includes preprocessing, feature extraction, a series of Mamba groups, and a reconstruction module.

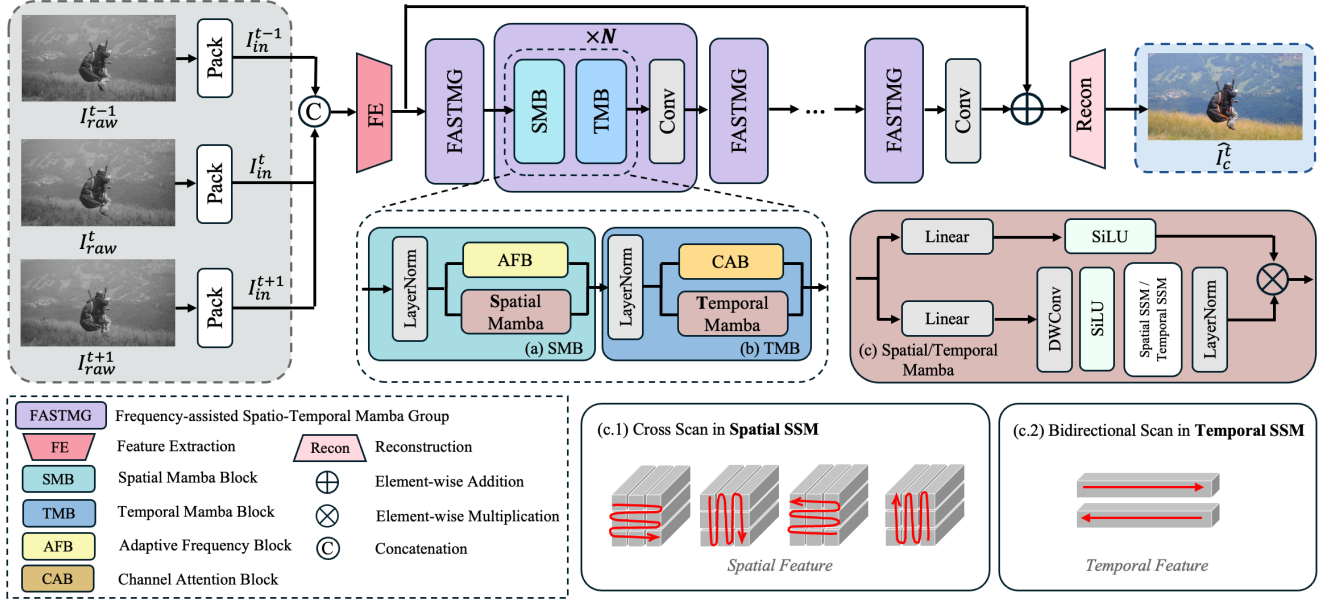


Figure 2. The overview and detailed structures of our proposed DemMamba.

For the preprocessing, the raw moiré images $\mathbf{I}_{raw}^{t+i} \in \mathbb{R}^{H \times W \times 3}$, $i \in \{-1, 0, +1\}$, where $H \times W$ represents the spatial resolution, are initially packed into the 4-channel RGGB format $\mathbf{I}_{in}^{t+i} \in \mathbb{R}^{\frac{H}{2} \times \frac{W}{2} \times 4}$, $i \in \{-1, 0, +1\}$. To address various moiré patterns across frames, we concatenate the packed inputs \mathbf{I}_{in}^{t+i} , $i \in \{-1, 0, +1\}$, and perform shallow feature extraction to obtain the shallow features $\mathbf{F}_0 \in \mathbb{R}^{\frac{H}{4} \times \frac{W}{4} \times C}$ through a single convolutional layer with a stride of two. Subsequently, we employ several Frequency-assisted Spatio-Temporal Mamba Groups (FASTMG) to learn the spatio-temporal features. Within each FASTMG, spatial and temporal dependencies are handled by specific modules. Each FASTMG consists of M SMB and M TMB organized sequentially to model both inter- and intra-frame relationships effectively, followed by a convolutional layer. In SMB, a 2-D selective scan is employed to capture spatial features, providing both a global effective receptive field and linear computational complexity relative to the input size. In conjunction with the spatial Mamba, we introduce an Adaptive Frequency Module (AFM) with an adaptive compressor in the frequency domain to attenuate the specific frequencies of moiré patterns. TMB processes flattened temporal sequences through simultaneous forward and backward SSMs, enhancing its capacity for temporal-aware processing. A Channel Attention Block (CAB) is embedded to further enhance temporal information interactions by exploiting inter-channel relationships among features. To preserve and integrate shallow and spatio-temporal features, we incorporate a global residual connection. Finally, the reconstruction module derives

$\hat{\mathbf{I}}_c^t$. The reconstruction module consists of several convolutional layers and a sub-pixel convolution layer to upsample the features, thus reconstructing the predicted clean image with height H and width W .

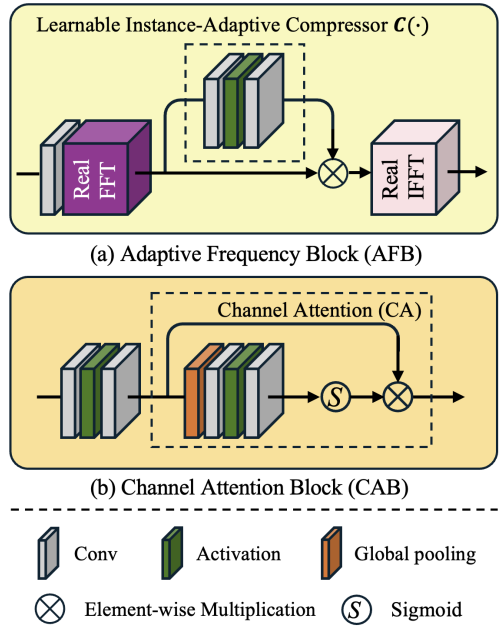


Figure 3. The structure of (a) AFB and (b) CAB.

3.2.1. Design of SMB

SMB, depicted in Fig. 2(a), is designed to establish spatial relationships of moiré patterns. Inspired by the success of Mamba in long-range modeling with linear complexity, we introduce the Spatial Mamba, shown in Fig. 2(c), to capture long-range dependencies in the spatial domain.

Following the standard Vision SSM design [29], the input feature $\mathbf{X} \in \mathbb{R}^{H \times W \times C}$ is processed through two parallel branches. In the first branch, the feature channels are expanded to λC by a linear layer, where λ is a pre-defined channel expansion factor, followed by depth-wise convolution, the SiLU activation function, the 2D-SSM layer, and LayerNorm. In the second branch, the feature channels are similarly expanded to λC using a linear layer, then processed with the SiLU activation function. Afterward, features from both branches are aggregated using the Hadamard product. The final output of the Spatial Mamba \mathbf{X}_{SM} is obtained by projecting the channel number back to C . The process in Spatial Mamba can be described as:

$$\begin{aligned}\mathbf{X}_1 &= \text{LN}(\text{2D-SSM}(\text{SiLU}(\text{DWConv}(\text{Linear}(\mathbf{X})))), \\ \mathbf{X}_2 &= \text{SiLU}(\text{Linear}(\mathbf{X})), \\ \mathbf{X}_{SM} &= \text{Linear}(\mathbf{X}_1 \odot \mathbf{X}_2),\end{aligned}\tag{5}$$

where \mathbf{X}_1 , \mathbf{X}_2 are the results from the two branches, DWConv denotes depth-wise convolution, and \odot is the Hadamard product.

To extend selective SSM to 2D spatial data, we follow [29] and introduce a 2D Selective Scan Module for cross scanning in Spatial SSM. As illustrated in Fig. 2(c.1), the 2D image feature is flattened and scanned along four directions: top-left to bottom-right, bottom-right to top-left, top-right to bottom-left, and bottom-left to top-right. Long-range dependencies are captured in each sequence using discrete state-space equations, and the sequences are then summed and reshaped to restore the 2D structure.

Considering that moiré patterns arise from frequency aliasing, we propose AFB to aid in the removal of moiré patterns in the frequency domain, operating in parallel with the Spatial Mamba. It is assumed that the frequency spectrum of moiré patterns tends to be relatively consistent within small patches. In signal processing, a band-reject filter allows most frequencies to pass unaltered while attenuating those within a specific range to very low levels. Given that different patches may require the attenuation of distinct frequencies, identifying a frequency prior for each moiré image patch is time-consuming. Consequently, as shown in Fig. 3(a), we construct a learnable instance-adaptive compressor $C(\cdot)$ in AFB, composed of several convolutional layers, to dynamically target and filter frequencies associated with moiré patterns while preserving the original image content. We use Real FFT and its inverse process to

apply $C(\cdot)$ in the frequency domain as:

$$\begin{aligned}\mathbf{X}_F &= F(\mathbf{X}), \\ \hat{\mathbf{X}} &= F^{-1}((C(\mathbf{X}_F)) \odot \mathbf{X}_F),\end{aligned}\tag{6}$$

where $F(\cdot)$ and $F^{-1}(\cdot)$ represent Real FFT and its inverse process, respectively.

Finally, the output of the SMB is produced through a weighted summation of the outputs from the Spatial Mamba and the AFB as:

$$\mathbf{X}_{SMB} = \mathbf{X}_{SM} + \alpha_1 \mathbf{X}_F,\tag{7}$$

where α_1 is a pre-defined weighting coefficient that enables the model to effectively reduce moiré patterns while maintaining overall visual quality and detail richness.

3.2.2. Design of TMB

TMB, depicted in Fig. 2(b), is designed to learn inter-channel relationships, which facilitates better utilization of neighboring information and preserves temporal consistency. Serving as the core structure of TMB, the Temporal Mamba is analogous to the aforementioned SMB but employs a different scanning strategy. Specifically, we opt for forward and backward scanning [58] on the flattened temporal sequences, given that there is only one dimension on the temporal axis, as illustrated in Fig. 2(c.2). This bidirectional scanning enables effective modeling of the interrelations across the temporal domain.

To enhance temporal information interactions, we introduce a CAB to exploit the inter-channel relationship among features. As shown in Fig. 3(b), CAB consists of two standard convolutional layers with a GELU activation and a channel attention (CA) module. For computational efficiency, the number of channel in the two convolutional layers is compressed by a constant γ . For an input feature with C channels, the number of channels in the output feature after the first convolutional layer is reduced to $\frac{C}{\gamma}$ and then expanded back to C channels through the second layer. Subsequently, a standard CA module [54] adaptively rescales channel-wise features. Finally, the output of the TMB can be computed by the weighted summation of the output from Temporal Mamba \mathbf{X}_{TM} and CAB \mathbf{X}_{CAB} as $\mathbf{X}_{TMB} = \mathbf{X}_{TM} + \alpha_2 \mathbf{X}_{CAB}$, where α_2 serves as the pre-defined weighting coefficient in TMB that enables the model to effectively integrate temporal dependencies while maintaining overall feature coherence.

3.3. Loss Function

We train our framework in an end-to-end manner with the overall training objective defined as:

$$\mathcal{L} = \|\hat{\mathbf{I}}_c^t - \mathbf{I}_c^t\|_1 + \|\Phi_l(\hat{\mathbf{I}}_c^t) - \Phi_l(\mathbf{I}_c^t)\|_1,\tag{8}$$

where \mathbf{I}_c^t represents the ground-truth moiré-free image of frame t . We employ L_1 loss alongside the perceptual

Table 1. Comparison with state-of-the-art image and video demoiréing methods for raw video demoiréing in terms of average PSNR, SSIM, LPIPS, and computing complexity. The best result is highlighted in bold and the second best is underlined.

	Method	PSNR \uparrow	SSIM \uparrow	LPIPS \downarrow	Parameters (M)	Inference time (s)
Image	RDNet	25.892	0.8939	0.1508	<u>2.722</u>	2.514
	RRID	27.283	0.9029	0.1168	2.374	<u>0.501</u>
Video	VDMoiré	27.277	0.9071	0.1044	5.836	1.057
	VDMoiré*	27.747	0.9116	0.0995	5.838	1.125
	DTNet	27.363	0.8963	0.1425	3.987	0.972
	DTNet*	27.892	0.9055	0.1135	3.368	1.050
	RawVD	<u>28.706</u>	0.9201	<u>0.0904</u>	6.585	1.247
	Ours	30.004	<u>0.9169</u>	0.0901	2.919	0.446

loss [17], which can closely reflect the human visual system’s perception of image quality. $\Phi_l(\cdot)$ denotes a set of VGG-16 layers.

4. Experiments

4.1. Experimental Setup

4.1.1. Dataset

We assess the effectiveness of our proposed DemMamba using the RawVDemoiré dataset [5], which consists of 300 clean raw source videos along with their corresponding moiré versions in the sRGB domain. RawVDemoiré dataset is divided into 250 videos for training and 50 videos for testing. Each video comprises 60 frames at a resolution of 720p (1080×720). Four camera-screen combinations are employed for dataset collection, resulting in frames with diverse moiré patterns. In addition, we utilize the raw image demoiréing dataset TMM22 [51] to verify the generalization ability of our method. TMM22 comprises 540 paired raw and sRGB images with ground truth for training and 408 pairs for testing, covering various recaptured scenes such as natural images, webpages, and documents. To facilitate the training and comparison process, patches sized 256×256 and 512×512 are cropped for the training and testing sets, respectively.

4.1.2. Training Details

DemMamba is trained using the AdamW optimizer, with β_1 set to 0.9 and β_2 set to 0.999. We employ a multistep learning rate schedule, with the learning rate initialized at 4×10^{-4} . DemMamba is trained for 50 epochs using a batch size of 8 on 2 NVIDIA Tesla H800 GPUs. For the structure in DemMamba, the numbers of FASTMG, SMB, and TMB are all set to 4. The weighting coefficient in SMB(α_1) and TMB(α_2) are both set to 0.5. In CAB, we set the squeeze factor γ between the two convolutional layers to 3.

4.2. Quantitative Results

We compare our approach with two raw image demoiréing methods, RDNet [51] and RRID [48], along with several video demoiréing methods: VDMoiré [6], DTNet [47] and

RawVD [5]. Since VDMoiré and DTNet are originally designed for video demoiréing in the sRGB domain, we have retrained them with raw inputs, adjusting the input channel number and inserting upsampling layers to adapt them to raw data. The revised versions are marked with an *. To evaluate the performance of our proposed DemMamba, we adopt the following three standard metrics to assess pixel-wise accuracy and the perceptual quality: PSNR, SSIM [43], and LPIPS [53]. Additionally, we assess model complexity by analyzing the number of parameters and inference time. To ensure a fair comparison, all models are fine-tuned using the default settings provided in their respective papers. We select the better results from the pre-trained and retrained models for comparison, providing an advantage over competing methods.

Table 1 presents the quantitative comparisons and computational complexity analysis on the RawVDemoiré dataset [5]. Our proposed DemMamba outperforms the second-best method, RawVD, by 1.3 dB in PSNR and 0.0003 in LPIPS. For SSIM, our method achieves the second-best result with a score of 0.9169, surpassing most of the compared methods. Regarding computational cost, our approach achieves effective demoiréing with the inference time of merely 0.446 seconds. Compared to previous methods, DemMamba demonstrates superiority with an acceptable parameter count of 2.919M, further highlighting the advantages of our approach.

Table 2. Quantitative comparison on TMM22 dataset.

Method	PSNR \uparrow	SSIM \uparrow	LPIPS \downarrow
DMCNN	23.54	0.885	0.154
DMCNN*	24.51	0.894	0.138
WDNet	22.33	0.802	0.166
WDNet*	23.08	0.815	0.149
ESDNet	26.77	0.927	0.089
ESDNet*	<u>27.48</u>	0.934	0.078
RDNet	26.16	0.921	0.091
RRID	27.24	0.929	0.098
RawVD	27.26	<u>0.935</u>	<u>0.075</u>
Ours	28.14	0.936	0.067

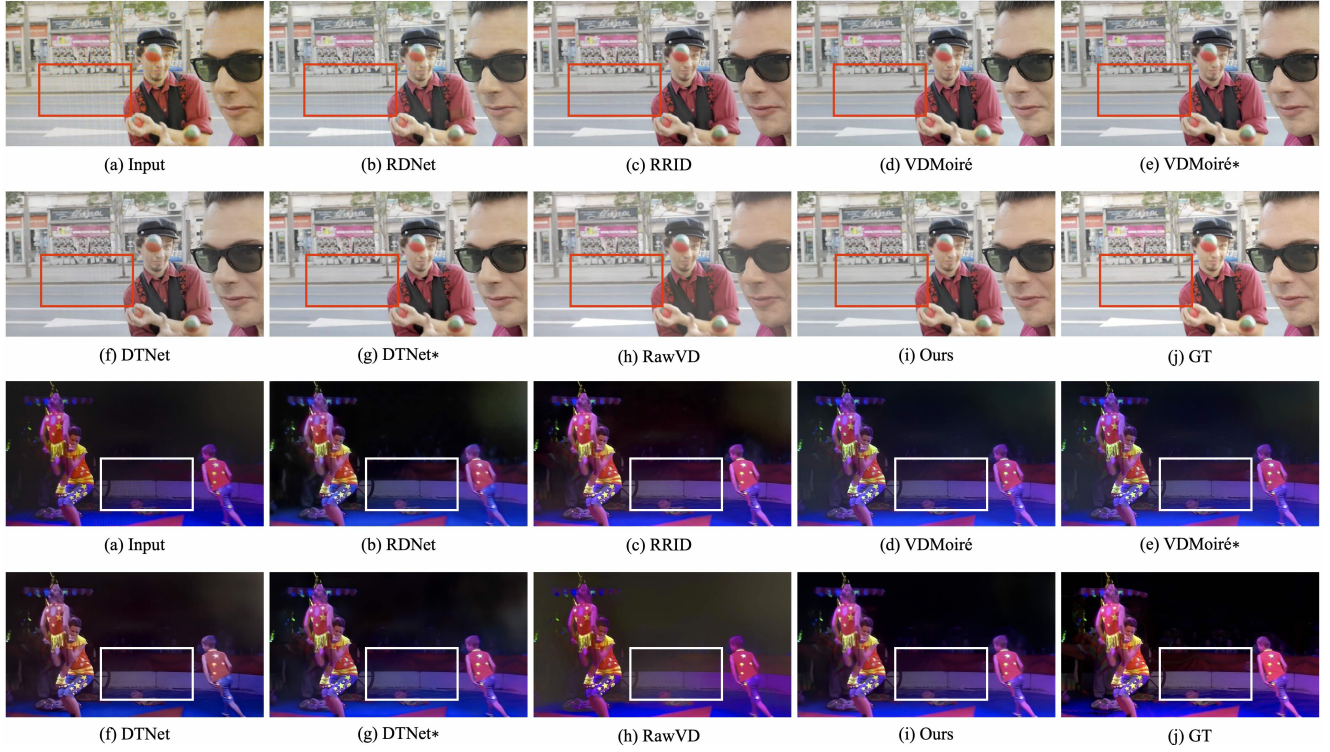


Figure 4. Qualitative comparison on raw video demoiréing RawVDmoiré dataset.

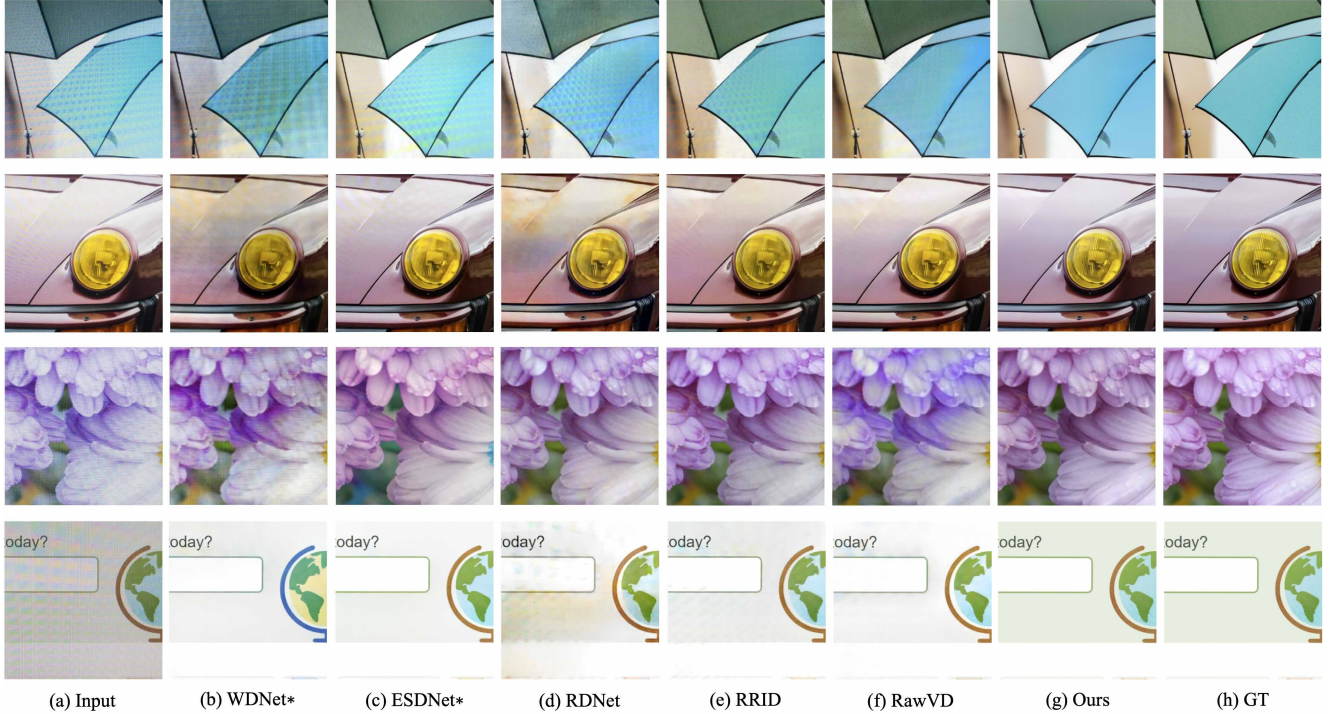


Figure 5. Qualitative comparison on raw image demoiréing TMM22 dataset.

To verify the generalization performance of our method, we conduct additional experiments on the raw image demoiréing dataset TMM22 [51]. To adapt to the TMM22 dataset, we input the same three frames into our model. In Table 2, we compare our method with several image demoiréing methods, including DMCNN [37], WD-Net [24], and ESDNet [50] (along with their corresponding raw input versions, denoted with *), as well as raw image demoiréing methods RDNet [51] and RRID [48], and the raw video demoiréing method RawVD [5]. Although DemMamba is initially designed for raw video demoiréing, it achieves the best performance on TMM22 dataset with a PSNR of 28.14 dB and an SSIM of 0.936. Regarding perceptual quality, DemMamba surpasses all the other methods with an LPIPS score of 0.067. The qualitative results on the TMM22 dataset further demonstrate the generalization capability of our method.

4.3. Qualitative Results

We present visual comparisons between our approach and existing methods in Fig. 4. The results demonstrate DemMamba’s ability in removing moiré patterns and correcting color deviations. In the first scenario, noticeable vertical moiré stripes appear in the light background regions. Unfortunately, the images restored by RDNet, RRID, VD-moiré and DTNet still exhibit remaining moiré patterns. Although RawVD can eliminate most of the moiré patterns, the resulting image tends to have a slight grayish bias. In contrast, DemMamba effectively removes the moiré patterns, preserves the original image details, and restores accurate colors. For the second scenario, which includes dark backgrounds with limited spatial details for model learning, our method still demonstrates stable demoiréing performance. DemMamba maintains higher texture accuracy, color fidelity, and structural coherence compared to other methods, underscoring its robustness in handling challenging low-light conditions.

Additionally, we present the qualitative comparison on raw image demoiréing dataset TMM22 in Fig. 5. In the first scene, which features a blue umbrella with moiré patterns, previous methods tend to leave residual moiré patterns in their restored images. In the final scene, we present a case of webpages affected by moiré patterns. Although some methods partially remove moiré patterns, they struggle to restore the original colors accurately. DemMamba’s ability to model long-range dependencies enables a more accurate restoration of colors, resulting in enhanced visual quality. Additional image and video comparisons are provided in the supplementary file.

4.4. Ablation Study

Table 3 shows an assessment of the effectiveness of our proposed DemMamba through ablation experiments with var-

Table 3. Ablation study for investigating the components in our proposed DemMamba.

Models	PSNR \uparrow	SSIM \uparrow
MambaIR	29.01	0.9119
w/o AFB	29.74	0.9161
w/o CAB	29.92	0.9167
all SMB	29.65	0.9156
all TMB	28.65	0.9118
DemMamba	30.00	0.9169

ious combinations of the foundational elements. Additionally, we introduce MambaIR [12] as a key baseline for comparison. Firstly, we validate the performance of MambaIR, which serves as an Mamba-based image restoration baseline. MambaIR achieves a PSNR of 29.01 dB in the raw video demoiréing task, demonstrating Mamba’s capability to manage long-term dependencies. However, the design of MambaIR limits its capacity in capturing temporal features, which is critical for video demoiréing. DemMamba employs alternating SMB and TMB to effectively capture intra- and inter-frame dependencies in raw videos affected by moiré patterns. To validate the effectiveness of this specific design, we replace one block type with the other. For instance, substituting all SMBs with TMBs results in a drastic PSNR decrease of approximately 1.4 dB. In addition, removing AFM and CAB respectively from the SMB and TMB leads to slight decreases of 0.26 dB and 0.08 dB in PSNR, underscoring the importance of the two modules. Incorporating all the designs, our complete model surpasses MambaIR by nearly 1 dB in PSNR, thereby affirming the efficacy of our frequency-assisted spatio-temporal Mamba.

5. Conclusion

We propose the innovative DemMamba network, an alignment-free raw video demoiréing method enhanced by frequency-assisted spatio-temporal Mamba. DemMamba adapts the Mamba framework to video restoration, strategically introducing SMB and TMB to model the inter- and intra-relationships, mitigating moiré patterns while ensuring temporal consistency. SMB captures global correlations within the spatial domain. Considering the frequency nature of moiré patterns, AFM is integrated as a learnable compressor, automatically adapting to and reducing specific moiré frequencies. TMB enhances the utilization of adjacent data to maintain temporal stability, supplemented by a CAB that strengthens temporal information integration. Extensive experiments demonstrate that our proposed DemMamba outperforms state-of-the-art methods both qualitatively and quantitatively.

References

[1] Jiesong Bai, Yuhao Yin, Qiyuan He, Yuanxian Li, and Xiaofeng Zhang. Retinexmamba: Retinex-based mamba for low-light image enhancement. *arXiv preprint arXiv:2405.03349*, 2024. 2

[2] Ali Behrouz, Michele Santacatterina, and Ramin Zabih. Mambamixer: Efficient selective state space models with dual token and channel selection. *arXiv preprint arXiv:2403.19888*, 2024. 3

[3] Guo Chen, Yifei Huang, Jilan Xu, Baoqi Pei, Zhe Chen, Zhiqi Li, Jiahao Wang, Kunchang Li, Tong Lu, and Limin Wang. Video mamba suite: State space model as a versatile alternative for video understanding. *arXiv preprint arXiv:2403.09626*, 2024. 3

[4] Xi Cheng, Zhenyong Fu, and Jian Yang. Multi-scale dynamic feature encoding network for image demoiréing. In *2019 IEEE/CVF International Conference on Computer Vision Workshop (ICCVW)*, pages 3486–3493. IEEE, 2019. 2

[5] Yijia Cheng, Xin Liu, and Jingyu Yang. Recaptured raw screen image and video demoiréing via channel and spatial modulations. *Advances in Neural Information Processing Systems*, 36, 2024. 1, 2, 3, 6, 8

[6] Peng Dai, Xin Yu, Lan Ma, Baoheng Zhang, Jia Li, Wenbo Li, Jiajun Shen, and Xiaojuan Qi. Video demoiréing with relation-based temporal consistency. In *Proceedings of the IEEE/CVF Conference on Computer Vision and Pattern Recognition*, pages 17622–17631, 2022. 1, 2, 6

[7] Rui Deng and Tianpei Gu. Cu-mamba: Selective state space models with channel learning for image restoration. *arXiv preprint arXiv:2404.11778*, 2024. 2

[8] Xingbo Dong, Wanyan Xu, Zhihui Miao, Lan Ma, Chao Zhang, Jiewen Yang, Zhe Jin, Andrew Beng Jin Teoh, and Jiajun Shen. Abandoning the bayer-filter to see in the dark. In *Proceedings of the IEEE/CVF Conference on Computer Vision and Pattern Recognition*, pages 17431–17440, 2022. 3

[9] Albert Gu and Tri Dao. Mamba: Linear-time sequence modeling with selective state spaces. *arXiv preprint arXiv:2312.00752*, 2023. 2, 3

[10] Albert Gu, Karan Goel, and Christopher Ré. Efficiently modeling long sequences with structured state spaces. *arXiv preprint arXiv:2111.00396*, 2021. 2

[11] Albert Gu, Isys Johnson, Karan Goel, Khaled Saab, Tri Dao, Atri Rudra, and Christopher Ré. Combining recurrent, convolutional, and continuous-time models with linear state space layers. *Advances in neural information processing systems*, 34:572–585, 2021. 3

[12] Hang Guo, Jinmin Li, Tao Dai, Zhihao Ouyang, Xudong Ren, and Shu-Tao Xia. Mambair: A simple baseline for image restoration with state-space model. In *European Conference on Computer Vision*, pages 222–241. Springer, 2025. 2, 3, 8

[13] Bin He, Ce Wang, Boxin Shi, and Ling-Yu Duan. Mop moire patterns using mopnet. In *ICCV*, pages 2424–2432, 2019. 2

[14] Bin He, Ce Wang, Boxin Shi, and Ling-Yu Duan. Fhde 2 net: Full high definition demoiréing network. In *Computer Vision–ECCV 2020: 16th European Conference, Glasgow, UK, August 23–28, 2020, Proceedings, Part XXII 16*, pages 713–729. Springer, 2020. 2

[15] Haofeng Huang, Wenhan Yang, Yueyu Hu, Jiaying Liu, and Ling-Yu Duan. Towards low light enhancement with raw images. *IEEE Transactions on Image Processing*, 31:1391–1405, 2022. 3

[16] Xin Jin, Ling-Hao Han, Zhen Li, Chun-Le Guo, Zhi Chai, and Chongyi Li. Dnf: Decouple and feedback network for seeing in the dark. In *Proceedings of the IEEE/CVF Conference on Computer Vision and Pattern Recognition*, pages 18135–18144, 2023. 3

[17] Justin Johnson, Alexandre Alahi, and Li Fei-Fei. Perceptual losses for real-time style transfer and super-resolution. In *Computer Vision–ECCV 2016: 14th European Conference, Amsterdam, The Netherlands, October 11–14, 2016, Proceedings, Part II 14*, pages 694–711. Springer, 2016. 6

[18] Rudolph Emil Kalman. A new approach to linear filtering and prediction problems. 1960. 2, 3

[19] Lingshun Kong, Jiangxin Dong, Ming-Hsuan Yang, and Jinshan Pan. Efficient visual state space model for image deblurring. *arXiv preprint arXiv:2405.14343*, 2024. 3

[20] Chenyang Lei and Qifeng Chen. Robust reflection removal with reflection-free flash-only cues. In *Proceedings of the IEEE/CVF Conference on Computer Vision and Pattern Recognition*, pages 14811–14820, 2021. 3

[21] Dong Li, Yidi Liu, Xueyang Fu, Senyan Xu, and Zheng-Jun Zha. Fouriermamba: Fourier learning integration with state space models for image deraining. *arXiv preprint arXiv:2405.19450*, 2024. 2, 3

[22] Wei-Tung Lin, Yong-Xiang Lin, Jyun-Wei Chen, and Kai-Lung Hua. Pixmamba: Leveraging state space models in a dual-level architecture for underwater image enhancement. *arXiv preprint arXiv:2406.08444*, 2024. 3

[23] Bolin Liu, Xiao Shu, and Xiaolin Wu. Demoiréing of camera-captured screen images using deep convolutional neural network. *arXiv preprint arXiv:1804.03809*, 2018. 2

[24] Lin Liu, Jianzhuang Liu, Shanxin Yuan, Gregory Slabaugh, Aleš Leonardis, Wengang Zhou, and Qi Tian. Wavelet-based dual-branch network for image demoiréing. In *Computer Vision–ECCV 2020: 16th European Conference, Glasgow, UK, August 23–28, 2020, Proceedings, Part XIII 16*, pages 86–102. Springer, 2020. 8

[25] Lin Liu, Shanxin Yuan, Jianzhuang Liu, Liping Bao, Gregory Slabaugh, and Qi Tian. Self-adaptively learning to demoiré from focused and defocused image pairs. *Advances in Neural Information Processing Systems*, 33:22282–22292, 2020. 2

[26] Lin Liu, Junfeng An, Shanxin Yuan, Wengang Zhou, Houqiang Li, Yanfeng Wang, and Qi Tian. Video demoiréing with deep temporal color embedding and video-image invertible consistency. *IEEE Transactions on Multimedia*, 2024. 1

[27] Mushui Liu, Jun Dan, Ziqian Lu, Yunlong Yu, Yingming Li, and Xi Li. Cm-unet: Hybrid cnn-mamba unet for remote sensing image semantic segmentation. *arXiv preprint arXiv:2405.10530*, 2024. 3

[28] Shuai Liu, Chenghua Li, Nan Nan, Ziyao Zong, and Ruixia Song. Mmdm: Multi-frame and multi-scale for image

demoiréing. In *Proceedings of the IEEE/CVF Conference on Computer Vision and Pattern Recognition Workshops*, pages 434–435, 2020. 2

[29] Yue Liu, Yunjie Tian, Yuzhong Zhao, Hongtian Yu, Lingxi Xie, Yaowei Wang, Qixiang Ye, Jianbin Jiao, and Yunfan Liu. Vmamba: Visual state space model. In *The Thirty-eighth Annual Conference on Neural Information Processing Systems*, 2024. 3, 5

[30] Fangzhou Luo, Xiaolin Wu, and Yanhui Guo. And: Adversarial neural degradation for learning blind image super-resolution. *Advances in Neural Information Processing Systems*, 36, 2024. 3

[31] Yuzhen Niu, Zhihua Lin, Wenxi Liu, and Wenzhong Guo. Progressive moire removal and texture complementation for image demoiréing. *IEEE Transactions on Circuits and Systems for Video Technology*, 2023. 2

[32] Yuzhen Niu, Rui Xu, Zhihua Lin, and Wenxi Liu. Stdnet: Spatio-temporal decomposition network for video demoiréing with sparse transformers. *IEEE Transactions on Circuits and Systems for Video Technology*, 2024. 1, 2

[33] Badri N Patro and Vijay S Agneeswaran. Simba: Simplified mamba-based architecture for vision and multivariate time series. *arXiv preprint arXiv:2403.15360*, 2024. 3

[34] Yuhui Quan, Haoran Huang, Shengfeng He, and Ruotao Xu. Deep video demoiréing via compact invertible dyadic decomposition. In *Proceedings of the IEEE/CVF International Conference on Computer Vision*, pages 12677–12686, 2023. 1, 2

[35] Yuan Shi, Bin Xia, Xiaoyu Jin, Xing Wang, Tianyu Zhao, Xin Xia, Xuefeng Xiao, and Wenming Yang. Vmambair: Visual state space model for image restoration. *arXiv preprint arXiv:2403.11423*, 2024. 2

[36] Binbin Song, Jiantao Zhou, Xiangyu Chen, and Shile Zhang. Real-scene reflection removal with raw-rgb image pairs. *IEEE Transactions on Circuits and Systems for Video Technology*, 2023. 3

[37] Yujing Sun, Yizhou Yu, and Wenping Wang. Moiré photo restoration using multiresolution convolutional neural networks. *IEEE Transactions on Image Processing*, 27(8):4160–4172, 2018. 2, 8

[38] Zifu Wan, Yuhao Wang, Silong Yong, Pingping Zhang, Simon Stepputtis, Katia Sycara, and Yaqi Xie. Sigma: Siamese mamba network for multi-modal semantic segmentation. *arXiv preprint arXiv:2404.04256*, 2024. 3

[39] Ce Wang, Bin He, Shengsen Wu, Renjie Wan, Boxin Shi, and Ling-Yu Duan. Coarse-to-fine disentangling demoiréing framework for recaptured screen images. *IEEE Transactions on Pattern Analysis and Machine Intelligence*, 2023. 1, 2

[40] Hailing Wang, Qiaoyu Tian, Liang Li, and Xiaojie Guo. Image demoiréing with a dual-domain distilling network. In *2021 IEEE International Conference on Multimedia and Expo (ICME)*, pages 1–6. IEEE, 2021. 2

[41] Jue Wang, Wentao Zhu, Pichao Wang, Xiang Yu, Linda Liu, Mohamed Omar, and Raffay Hamid. Selective structured state-spaces for long-form video understanding. In *Proceedings of the IEEE/CVF Conference on Computer Vision and Pattern Recognition*, pages 6387–6397, 2023. 3

[42] Xintao Wang, Kelvin CK Chan, Ke Yu, Chao Dong, and Chen Change Loy. Edvr: Video restoration with enhanced deformable convolutional networks. In *Proceedings of the IEEE/CVF conference on computer vision and pattern recognition workshops*, pages 0–0, 2019. 2

[43] Zhou Wang, Alan C Bovik, Hamid R Sheikh, and Eero P Simoncelli. Image quality assessment: from error visibility to structural similarity. *IEEE transactions on image processing*, 13(4):600–612, 2004. 6

[44] Hongtao Wu, Yijun Yang, Huihui Xu, Weiming Wang, Jinni Zhou, and Lei Zhu. Rainmamba: Enhanced locality learning with state space models for video deraining. *arXiv preprint arXiv:2407.21773*, 2024. 3

[45] Zeyu Xiao, Zhihe Lu, and Xinchao Wang. P-bic: Ultra-high-definition image demoiréing via patch bilateral compensation. In *ACM Multimedia 2024*, 2020. 2

[46] Wenzhu Xing and Karen Egiazarian. End-to-end learning for joint image demosaicing, denoising and super-resolution. In *Proceedings of the IEEE/CVF conference on computer vision and pattern recognition*, pages 3507–3516, 2021. 3

[47] Shuning Xu, Binbin Song, Xiangyu Chen, and Jiantao Zhou. Direction-aware video demoiréing with temporal-guided bilateral learning. In *Proceedings of the AAAI Conference on Artificial Intelligence*, pages 6360–6368, 2024. 1, 2, 6

[48] Shuning Xu, Binbin Song, Xiangyu Chen, Xina Liu, and Jiantao Zhou. Image demoiréing in raw and srgb domains. In *European Conference on Computer Vision*, pages 108–124. Springer, 2025. 1, 2, 3, 6, 8

[49] Chenhongyi Yang, Zehui Chen, Miguel Espinosa, Linus Ericsson, Zhenyu Wang, Jiaming Liu, and Elliot J Crowley. Plainmamba: Improving non-hierarchical mamba in visual recognition. *arXiv preprint arXiv:2403.17695*, 2024. 3

[50] Xin Yu, Peng Dai, Wenbo Li, Lan Ma, Jiajun Shen, Jia Li, and Xiaojuan Qi. Towards efficient and scale-robust ultra-high-definition image demoiréing. In *Computer Vision–ECCV 2022: 17th European Conference, Tel Aviv, Israel, October 23–27, 2022, Proceedings, Part XVIII*, pages 646–662. Springer, 2022. 2, 8

[51] Huanjing Yue, Yijia Cheng, Yan Mao, Cong Cao, and Jingyu Yang. Recaptured screen image demoiréing in raw domain. *IEEE Transactions on Multimedia*, 2022. 1, 3, 6, 8

[52] Huanjing Yue, Zhiming Zhang, and Jingyu Yang. Real-rawvrs: Real-world raw video super-resolution with a benchmark dataset. In *European Conference on Computer Vision*, pages 608–624. Springer, 2022. 3

[53] Richard Zhang, Phillip Isola, Alexei A Efros, Eli Shechtman, and Oliver Wang. The unreasonable effectiveness of deep features as a perceptual metric. In *Proceedings of the IEEE conference on computer vision and pattern recognition*, pages 586–595, 2018. 6

[54] Yulun Zhang, Kunpeng Li, Kai Li, Lichen Wang, Bineng Zhong, and Yun Fu. Image super-resolution using very deep residual channel attention networks. In *Proceedings of the European conference on computer vision (ECCV)*, pages 286–301, 2018. 5

[55] Yuxin Zhang, Mingbao Lin, Xunchao Li, Han Liu, Guozhi Wang, Fei Chao, Shuai Ren, Yafei Wen, Xiaoxin Chen, and

Rongrong Ji. Real-time image demoirreing on mobile devices. *arXiv preprint arXiv:2302.02184*, 2023. [2](#)

[56] Zou Zhen, Yu Hu, and Zhao Feng. Freqmamba: Viewing mamba from a frequency perspective for image deraining. *arXiv preprint arXiv:2404.09476*, 2024. [3](#)

[57] Bolun Zheng, Shanxin Yuan, Gregory Slabaugh, and Ales Leonardis. Image demoirreing with learnable bandpass filters. In *Proceedings of the IEEE/CVF Conference on Computer Vision and Pattern Recognition*, pages 3636–3645, 2020. [2](#)

[58] Lianghui Zhu, Bencheng Liao, Qian Zhang, Xinlong Wang, Wenyu Liu, and Xinggang Wang. Vision mamba: Efficient visual representation learning with bidirectional state space model. *arXiv preprint arXiv:2401.09417*, 2024. [2](#), [3](#), [5](#)

[59] Qinfeng Zhu, Yuan Fang, Yuanzhi Cai, Cheng Chen, and Lei Fan. Rethinking scanning strategies with vision mamba in semantic segmentation of remote sensing imagery: An experimental study. *arXiv preprint arXiv:2405.08493*, 2024. [3](#)